

Coulomb Drag in Graphene

Wang-Kong Tse¹, Ben Yu-Kuang Hu^{1,2}, and S. Das Sarma¹

¹*Condensed Matter Theory Center, Department of Physics,
University of Maryland, College Park, Maryland 20742 and*

²*Department of Physics, University of Akron, Akron, Ohio 44325-4001*

We study the Coulomb drag between two single graphene sheets in intrinsic and extrinsic graphene systems with no interlayer tunneling. The general expression for the nonlinear susceptibility appropriate for single-layer graphene systems is derived using the diagrammatic perturbation theory, and the corresponding exact zero-temperature expression is obtained analytically. We find that, despite the existence of a non-zero conductivity in an intrinsic graphene layer, the Coulomb drag between intrinsic graphene layers vanishes at all temperatures. In extrinsic systems, we obtain numerical results and an approximate analytical result for the drag resistivity ρ_D , and find that ρ_D goes as T^2 at low temperature T , as $1/d^4$ for large bilayer separation d and $1/n^3$ for high carrier density n . We also discuss qualitatively the effect of plasmon-induced enhancement on the Coulomb drag, which should occur at a temperature of the order of or higher than the Fermi temperature.

PACS numbers:

I. INTRODUCTION

With the recent advent of the experimental fabrication of a single layer of graphene, the electronic and transport properties of this newly discovered material have been intensively studied both experimentally^{1,2} and theoretically^{3,4}. Whereas electronic structure experiments have revealed detailed subtle many-body effects on the graphene energy spectrum, transport experiments have also revealed some apparently unusual features of graphene transport properties, most notably, that the conductivity has a non-zero minimum value around zero bias gate voltage. Up to now, the transport experiments performed have been focused only on the longitudinal and Hall transport properties (in both weak and strong magnetic fields, including the quantum Hall regime) and weak localization, where all of these phenomena depend essentially only on the physics of scattering of individual single quasiparticle from impurities with electron-electron many-body interaction effect playing the role of a small quantitative correction. In two-dimensional electron gas (2DEG) semiconductor bilayer structures (e.g. modulation-doped GaAs/Al_xGa_{1-x}As double quantum wells), electron-electron scattering between the 2DEG layers give rise to the effect of Coulomb drag where a ‘drag’ current is induced purely from the momentum exchanges through interlayer electron-electron scattering events. One measures the effect of Coulomb drag by the drag resistivity ρ_D , which is defined by the induced drag electric field in the open-circuited passive layer per unit applied current density in the active layer. In high-mobility samples where the disorder is weak, ρ_D goes as T^2 at low temperatures T , and as $1/d^4$ for large bilayer separation d (Refs. 5,6).

In this paper, we investigate the Coulomb drag in graphene ‘bilayer’ systems with no interlayer tunneling, considering both the intrinsic (chemical potential $\mu = 0$) and extrinsic ($\mu \neq 0$) cases. We emphasize right in the beginning so that there is no semantic confusion what

we mean by the terminology ‘bilayer’ graphene. Our ‘bilayer’ graphene is two isolated parallel 2D graphene monolayers separated by a distance d , with *no* interlayer tunneling. The electronic structure of each graphene monolayer is thus unaffected by having the other layer. Each graphene layer is assumed to have its own variable carrier density in the extrinsic case. Our system is thus different from the ordinary bilayer graphene where $d \sim 1 - 5 \text{ \AA}$ with strong interlayer tunneling. Throughout this paper, we shall also use the terms ‘undoped’ and ‘doped’ interchangeably with ‘intrinsic’ and ‘extrinsic’ respectively; keeping in mind that in experiments the chemical potential can be changed by both chemical doping and gating with an applied voltage. The Coulomb drag in graphene is interesting not only because it is a novel material with a linear energy spectrum, but also because it only spans a thickness of a single carbon atom, the electrons are much more confined along the perpendicular direction comparing with 2DEG in a quantum well, where the finite width thickness has to be taken into account in any quantitative comparison with experiments. Thus, the Coulomb drag phenomenon in graphene is expected to be theoretically very well accounted for with two zero-thickness graphene sheets. In addition, tunneling is only appreciable when the the out-of-plane π orbitals from the two graphene sheets start to overlap with each other at an interlayer distance d of a few angstroms ($d \simeq 3.5 \text{ \AA}$ in naturally occurring graphite), making it possible to study the effect of Coulomb drag for an interlayer separation d down to a few tens of angstroms, about an order of magnitude smaller than is possible in the usual double quantum well systems without appreciable tunneling.

II. FORMALISM

Graphene has a real-space honeycomb lattice structure with two interpenetrating sublattices, giving a honey-

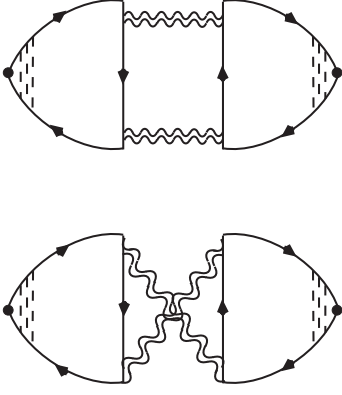


FIG. 1: Diagrams contributing to the drag resistivity Eq. (3). The double wavy lines represent the screened interlayer Coulomb potential Eq. (4) and the vertices on the left and on the right denote charge current in the two layers. Dashed vertical lines next to the vertices denote impurity vertex correction to the charge current.

comb reciprocal space structure with the Brillouin zone forming a hexagon. At each of these corners where the high symmetry point is denoted as K or K', the energy dispersion is linear and the effective low-energy Hamiltonian at the vicinity of these K and K' points is given by $H_0 = v\hat{\sigma} \cdot \mathbf{k}$. The eigenenergy is $\epsilon_{\mathbf{k}\lambda} = \lambda vk$, where the chirality label $\lambda = \pm 1$ describes conduction band ($\lambda = 1$) and valence band ($\lambda = -1$) spectra. Throughout this paper we choose $\hbar = 1$ unless it is written out explicitly. The transformation which diagonalizes the Hamiltonian is a local transformation, dependent on the momentum \mathbf{k} through $\tan\phi_{\mathbf{k}} = k_y/k_x$:

$$U_{\mathbf{k}} = \frac{1}{\sqrt{2}} \begin{bmatrix} 1 & 1 \\ e^{i\phi_{\mathbf{k}}} & -e^{i\phi_{\mathbf{k}}} \end{bmatrix}. \quad (1)$$

The central quantity in the Coulomb drag problem is the nonlinear susceptibility^{7,8,9}, Γ :

$$\Gamma(\mathbf{q}, \omega) = \int \frac{d\varepsilon}{2\pi i} [n_F(\varepsilon + \omega) - n_F(\varepsilon)] \sum_{\mathbf{k}} \text{tr} \left\{ [G_{\mathbf{k}-\mathbf{q}}^A(\varepsilon) - G_{\mathbf{k}-\mathbf{q}}^R(\varepsilon)] G_{\mathbf{k}}^A(\varepsilon + \omega) \mathbf{J}(\mathbf{k}) G_{\mathbf{k}}^R(\varepsilon + \omega) \right\} + \{\mathbf{q}, \omega \rightarrow -\mathbf{q}, -\omega\}, \quad (2)$$

where $G_{\mathbf{k}}^{R,A}(\varepsilon) = (\varepsilon - H_0 \pm i/2\tau)^{-1}$ denotes, within the Born approximation for the self-energy, the impurity-averaged retarded/advanced Green function, τ the lifetime due to impurity scattering, \mathbf{J} the charge current vertex, n_F the Fermi function and 'tr' the trace. In the rest of this paper, we shall simply denote the x -components of Γ and \mathbf{J} as Γ and J . The drag conductivity, diagrammatically shown in Fig. 1, is given by^{7,8,9}

$$\sigma_D = \frac{1}{16\pi k_B T} \sum_{\mathbf{q}} \int_0^\infty \frac{d\omega}{\sinh^2(\hbar\omega/2k_B T)} \Gamma_1(\mathbf{q}, \omega) \Gamma_2(\mathbf{q}, \omega) |U_{12}(\mathbf{q}, \omega)|^2, \quad (3)$$

here subscripts '1' and '2' are the labels for the two single-layer graphene, U_{12} is the screened interlayer potential, which in the random phase approximation (RPA) is given by

$$U_{12}(\mathbf{q}, \omega) = \frac{V(\mathbf{q})e^{-qd}}{[1 + \Pi_1 V(\mathbf{q})][1 + \Pi_2 V(\mathbf{q})] - \Pi_1 \Pi_2 V^2(\mathbf{q})e^{-2qd}}, \quad (4)$$

where d is the interlayer spacing, $V(\mathbf{q}) = 2\pi e^2/q$ is the bare Coulomb potential, $\Pi(\mathbf{q}, \omega)$ is the graphene polarizability⁴. Instead of the drag conductivity, in experiments one measures the drag resistivity ρ_D which is defined as (here W and L are the width and length of the sample, respectively) $\rho_D \equiv (W/L)(V_2/I_1)$, the ratio of the induced voltage in the passive layer V_2 to the applied current in the active layer I_1 . The drag resistivity is then obtained from the drag conductivity as $\rho_D = \sigma_D/(\sigma_{L1}\sigma_{L2} - \sigma_D^2) \simeq \sigma_D/\sigma_{L1}\sigma_{L2}$, where $\sigma_{L1,2}$ is the longitudinal conductivity of the individual layer 1 or 2.

In this paper, we shall restrict ourselves to the Boltzmann regime ($\omega\tau \gg 1$ or $ql \gg 1$, where $l = v\tau$ is the mean free path) corresponding to weak impurity scattering, which is the case relevant to actual experimental situations where high-mobility samples with dilute impurities are used. The longitudinal current for the graphene Hamiltonian is $\mathbf{J} = e\partial H_0/\partial \mathbf{k} = ev\hat{\sigma}$. In the presence of impurities, vertex correction to the current is taken into account within the impurity ladder approximation, which gives the impurity-dressed current vertex as $\mathbf{J} = (\tau_{\text{tr}}/\tau)ev\hat{\sigma}$, where the transport time τ_{tr} for graphene is given by

$$\tau_{\text{tr}}^{-1} = \pi \sum_{\mathbf{k}'} n_i |u_i(\mathbf{k} - \mathbf{k}')|^2 (1 - \cos^2\theta_+) \delta(\epsilon_{\mathbf{k}+} - \epsilon_{\mathbf{k}'+}) \Big|_{k=k_F}, \quad (5)$$

with n_i and u_i being respectively the impurity density and impurity potential; $\theta_+ = \phi_{\mathbf{k}+\mathbf{q}} - \phi_{\mathbf{k}}$ being the scattering angle from momentum \mathbf{k} to $\mathbf{k} + \mathbf{q}$. We have given Eq. (5) for the transport time here only for the purpose of completeness, as our final results for the drag resistivity do not depend on τ_{tr} .

Following Ref. 9, we express the nonlinear susceptibility Eq. (2) as

$$\Gamma(\mathbf{q}, \omega) = \tau \sum_{\lambda, \lambda' = \pm} \sum_{\mathbf{k}} \left[\tilde{J}_{\lambda\lambda}(\mathbf{k} + \mathbf{q}) - \tilde{J}_{\lambda'\lambda'}(\mathbf{k}) \right] \text{Im} \left\{ (1 + \lambda\lambda' \cos\theta_+) \frac{n_F(\epsilon_{\mathbf{k}\lambda'}) - n_F(\epsilon_{\mathbf{k}+\mathbf{q}\lambda})}{\omega + \epsilon_{\mathbf{k}\lambda'} - \epsilon_{\mathbf{k}+\mathbf{q}\lambda} + i0^+} \right\}. \quad (6)$$

where $\tilde{J}(\mathbf{k}) = U_{\mathbf{k}}^\dagger \mathbf{J} U_{\mathbf{k}}$ is the impurity-dressed charge current vertex expressed in the chiral basis. Eq. (6) is different from the nonlinear susceptibility for regular 2DEG with quadratic spectrum in two ways: (1) there are contributions to the electron-hole excitations coming from intraband transitions ($\lambda = \lambda'$) and interband transitions ($\lambda \neq \lambda'$); (2) there is an additional factor

$(1 \pm \cos\theta_+)/2$, which derives from the Berry phase structure of the graphene Hamiltonian. Furthermore, the nonlinear susceptibility Eq. (6) is not directly proportional to the imaginary part of the polarizability as in regular 2DEG, because here the current $\tilde{\mathbf{J}}(\mathbf{k})$ is not directly proportional to the momentum \mathbf{k} . Eq. (6) has the same formal structure as in the case of a regular 2DEG with Rashba/Dresselhaus spin-orbit coupling⁹, where $\lambda = \pm 1$ describes the two spin-split bands. The finite off-diagonal components of $\tilde{\mathbf{J}}$ do not contribute to the nonlinear susceptibility, and only the diagonal components $\tilde{J}_{\lambda\lambda} = \lambda(\tau_{\text{tr}}/\tau)ev \cos\phi_{\mathbf{k}}$ enter into the expression Eq. (6), corresponding to electrons moving in the conduction band ($\lambda = 1$) with a velocity of constant magnitude $(\tau_{\text{tr}}/\tau)\mathbf{v}$ and valence band ($\lambda = -1$) with $-(\tau_{\text{tr}}/\tau)\mathbf{v}$. In the following, we consider the Coulomb drag between intrinsic graphene layers and extrinsic graphene layers separately.

III. DRAG IN INTRINSIC GRAPHENE SYSTEMS

For the case where the graphene layers are undoped $\mu = 0$, we first state the main result: the drag conductivity between two intrinsic graphene layers, or between one extrinsic and one intrinsic graphene layers, is identically zero. This is not at first sight a trivial consequence of zero doping if one recalls there is a finite conductivity (so-called the ‘‘minimum conductivity’’) at zero doping in graphene. A physical explanation and a general argument for the reason why this is so is in order. When the Fermi level is at the Dirac point, the only process for electron-hole pair creation will be interband electron excitation from the valence band to the conduction band by which equal numbers of electrons and holes are created. In the mechanism of Coulomb drag, the applied electric field drives the electrons (or holes) in the active layer in the, say, positive (negative) direction; through Coulomb scattering, momentum is transferred to the passive layer, which drives the carriers (regardless of whether these are electrons or holes) in the same direction as the momentum transfer. In doped systems where there is only one type of carrier (either electron or hole), this gives a finite drag current in the passive layer. Now, in undoped systems where a perfect electron-hole symmetry exists, there are two cases for consideration: (1) If the active layer is undoped, equal numbers of electrons and holes in the active layer will be driven in the opposite direction by the applied electric field, and the net momentum transfer is thus zero. There will be no drag regardless of what the passive layer is. (2) If the active layer is doped while the passive layer is undoped, equal numbers of electrons and holes in the passive layer will be driven in the same direction by the momentum transfer, therefore resulting in a vanishing drag current. The conclusion of these qualitative considerations amounts to a vanishing nonlinear susceptibility $\Gamma(q, \omega) = 0$, which we now proof as fol-

lows. We first make a change of the integration variable $\mathbf{k}' = -\mathbf{k}$ in Eq. (6), and use time-reversal symmetry to obtain

$$\Gamma(\mathbf{q}, \omega) = \tau \sum_{\lambda, \lambda' = \pm} \sum_{\mathbf{k}'} \left[-\tilde{J}_{\lambda\lambda}(\mathbf{k}' - \mathbf{q}) + \tilde{J}_{\lambda'\lambda'}(\mathbf{k}') \right] \text{Im} \left\{ (1 + \lambda\lambda' \cos\theta_-) \frac{n_F(\epsilon_{\mathbf{k}'\lambda'}) - n_F(\epsilon_{\mathbf{k}' - \mathbf{q}\lambda})}{\omega + \epsilon_{\mathbf{k}'\lambda'} - \epsilon_{\mathbf{k}' - \mathbf{q}\lambda} + i0^+} \right\}, \quad (7)$$

where $\theta_- = \phi_{\mathbf{k}} - \phi_{\mathbf{k} - \mathbf{q}}$. This is so far general. Next we impose the symmetry requirements of the bands about $\epsilon = 0$, i.e. $\epsilon_{\mathbf{k}'\lambda} = -\epsilon_{\mathbf{k}'\lambda}$ and $\tilde{J}_{\mathbf{k}'\lambda} = -\tilde{J}_{\mathbf{k}'\lambda}$, and then change the band labels as $r' = -\lambda$, $r = -\lambda'$ in Eq. (7). Finally, using the relation $n_F(\epsilon_{\mathbf{k}'r}) = 1 - n_F(\epsilon_{\mathbf{k}'r})$ valid for the undoped case $\mu = 0$, we arrive at $\Gamma = -\Gamma$, i.e. $\Gamma(q, \omega) \equiv 0$. This result holds true for any type of spectrum where the two bands have a mirror symmetry across $\epsilon = 0$, and any bilayer system with one or both of the layers having such a band symmetry with zero doping always results in an overall vanishing drag at all temperatures.

IV. DRAG IN EXTRINSIC GRAPHENE SYSTEMS

We now move on to the drag between finite-doped graphene layers. We first provide the exact analytical results for the nonlinear susceptibility Eq. (6) with Fermi energy $\epsilon_F > 0$ (in the following $x = q/k_F$ and $y = \omega/\epsilon_F$, and $\tilde{\Gamma} = \Gamma/(2ek_F\tau/\pi)$):

$$\tilde{\Gamma}(x, y) = \tilde{\Gamma}_{\text{intra}}\theta(x - y) + \tilde{\Gamma}_{\text{inter}}\theta(y - x), \quad (8)$$

where θ is the unit step function, $\tilde{\Gamma}_{\text{intra}}$ is the intraband contribution to the nonlinear susceptibility given by the terms with $\lambda = \lambda'$ in Eq. (6),

$$\begin{aligned} \tilde{\Gamma}_{\text{intra}}(x, y) = & \frac{1}{4x} \sqrt{x^2 - y^2} \left\{ 2\sqrt{(y+x-2)(y-x-2)} \right. \\ & - \sqrt{x^2 - y^2} \left[\tan^{-1} \left[\frac{\sqrt{(y+x-2)(y-x-2)}\sqrt{x^2 - y^2}}{x^2 - 2 - (y-2)y} \right] \right. \\ & \left. \left. + \pi\theta[y(y-2) - x^2 + 2] \right] \right\} \theta(2-x-y) - \{y \rightarrow -y\}, \quad (9) \end{aligned}$$

and $\tilde{\Gamma}_{\text{inter}}$ is the interband contribution given by the terms with $\lambda \neq \lambda'$ in Eq. (6),

$$\begin{aligned} \tilde{\Gamma}_{\text{inter}}(x, y) = & -\frac{1}{4x} \sqrt{y^2 - x^2} \left\{ 2\sqrt{(x+y-2)(x-y+2)} \right. \\ & + \sqrt{y^2 - x^2} \left[\tan^{-1} \left[\frac{\sqrt{(x+y-2)(x-y+2)}\sqrt{y^2 - x^2}}{x^2 - 2 - (y-2)y} \right] \right. \\ & \left. \left. - \pi\theta[x^2 - 2 - (y-2)y] \right] \right\} \theta(x+y-2)\theta(x-y+2). \quad (10) \end{aligned}$$

The intraband contribution corresponds to electron-hole excitations in the vicinity of the Fermi level within the conduction band, which occur at $\omega < vq$; whereas the

interband contribution corresponds to electron-hole excitations from the valence band to the conduction band, which occur at $\omega > vq$. Using Eqs. (3), (9)-(10) and the expression for the graphene polarizability⁴, we have calculated numerically the drag resistivity ρ_D for different values of interlayer distance d and density n (Fig. 3). Before we proceed to discuss our numerical results, it is instructive to obtain an analytical formula for the drag resistivity under certain approximations. To this end, we first define the standard dimensionless parameter for the excitation energy $u = y/x = \omega/vq$ in the Fermi liquid theory, which is the ratio of the phase velocity of the excitation ω/q to the quasiparticle velocity v . At low temperatures and with large interlayer separation, the dominant contribution to the drag conductivity Eq. (3) comes from region with small q and ω , consequently the nonlinear susceptibility can be evaluated in the limits of long wavelength $x \ll 1$ and low energy $u \ll 1$, allowing a closed-form expression for $\Gamma(q, \omega)$ to be extracted. The interband ($\lambda \neq \lambda'$) contribution in Eq. (6) is in general smaller than the intraband ($\lambda = \lambda'$) contribution by an order $\mathcal{O}(x^2)$, and vanishes in the limit $u \ll 1$ as seen from Eq. (8). This is because, in the presence of a finite Fermi level, electrons take more energy to transition from the valence band to the conduction band (interband) than to transition within the conduction band (intraband), and with a small excitation energy the channel of interband transition becomes inaccessible. With the above assumptions, Eq. (6) can be evaluated as

$$\begin{aligned} \tilde{\Gamma}(x, y = ux) = \tilde{\Gamma}_{\text{intra}} = -4u \left[(1 - ux) \frac{t_+ \theta(1 - |t_+|)}{\sqrt{1 - t_+^2}} \right. \\ \left. - (1 + ux) \frac{t_- \theta(1 - |t_-|)}{\sqrt{1 - t_-^2}} \right] \simeq -4ux \end{aligned} \quad (11)$$

where $t_{\pm} = u \pm x(1 - u^2)/2$. Eq. (11) is larger than the corresponding expression for the nonlinear susceptibility in regular 2DEG by a factor of 4, due to an extra 2×2 degrees of freedom coming from the spin and valley degeneracies in graphene, in addition to the two sublattice degrees of freedom which give rise to the conduction and valence bands.

The longitudinal conductivity can be obtained from the impurity-dressed current $\mathbf{J} = (\tau_{\text{tr}}/\tau)ev\hat{\sigma}$ using the Kubo formula to give $\sigma_L = e^2\nu D$, where $\nu = 2k_F/\pi v$ is the graphene density of states and $D = v^2\tau_{\text{tr}}/2$ is the diffusion constant. This Kubo formula result is identical with the Boltzmann theory result $\sigma_L = (e^2/\hbar)2\varepsilon_F\tau_{\text{tr}}/h$. Incidentally, for short-range impurities the transport time is related to the lifetime simply by $\tau_{\text{tr}} = 2\tau$ due to the suppression of backscattering from impurities in graphene. There are two types of disorder in substrate-mounted graphene, one being the charged impurities coming from the substrate; and the other being the neutral impurities intrinsic to the graphene layer itself. In theory, the type of disorder essentially boils down to the

expression of the transport time τ_{tr} in σ_L , which yield different types of functional dependence of the conductivity σ_L on the carrier density. In experiments, the conductivity is observed to increase linearly with density, a fact alluding to the dominance of the charged impurity scattering in substrate-mounted graphene samples. We emphasize that this dependence on different types of disorder does not affect the expression of the drag resistivity as the transport time τ_{tr} is explicitly canceled out between σ_D and $\sigma_{L1}\sigma_{L2}$. Therefore, our calculation and conclusions apply equally to bilayer systems with substrate-mounted (where charged impurity scattering plays the more dominant role) or suspended graphene samples (where there is only neutral impurity scattering).

In the expression of the drag conductivity Eq. (3), the dominant contribution of the integral comes from the region where $qd \lesssim 1$, and for large interlayer separation d satisfying $d^{-1} \ll k_F, q_{\text{TF}}$, the interlayer potential Eq. (4) can be approximated as $U_{12} \simeq q/4\pi e^2 \sinh(qd)\Pi_1\Pi_2$. Furthermore, the denominator $\sinh^2(\omega/2k_B T)$ in Eq. (3) also restricts the upper limit of the ω integral to a few $\sim k_B T$, therefore at low temperatures only small values of ω/ε_F contribute to Eq. (3). As a consequence, the polarizability for doped graphene can be approximated by the static screening result $\Pi(q, \omega) \simeq \nu$. Now, using Eq. (11) for the nonlinear susceptibility, the drag resistivity is obtained as

$$\rho_D = \frac{h}{e^2} \frac{\pi\zeta(3)}{32} \frac{(k_B T)^2}{\varepsilon_{F1}\varepsilon_{F2}} \frac{1}{(q_{\text{TF}1}d)(q_{\text{TF}2}d)} \frac{1}{(k_{F1}d)(k_{F2}d)}, \quad (12)$$

where $q_{\text{TF}} = 4e^2k_F/v$ is the Thomas-Fermi wavenumber for extrinsic graphene³. The drag resistivity Eq. (12), valid for low temperatures $T \ll T_F$ and high density and/or large interlayer separation $k_F d \gg 1$, has exactly the same form as in the regular 2DEG drag, exhibiting the same dependences of temperature ($\sim T^2$), interlayer separation ($\sim 1/d^4$) and density ($\sim (n_1 n_2)^{-3/2}$).

Our numerical calculations and analytical results Eq. (12) are compared in Fig. 2, showing that Eq. (12) becomes an increasingly accurate approximation to the full numerical results with increasing values of $k_F d$. The fact that the exact numerical results shown in Fig. 2 disagree more strongly with the analytic result of Eq. (12) for smaller values of $k_F d$ is understandable, since the analytic formula given in Eq. (12) applies only in the asymptotic $k_F d \gg 1$ limit, and for lower carrier density and/or interlayer separation, Eq. (12) simply does not apply. In particular, for $k_F d = 1$, the exact numerical result for Coulomb drag is a factor of 4 larger than that given by Eq. (12). This trend of an increasing quantitative failure of the asymptotic analytic drag formula for lower values of $k_F d$ has also been noted in the literature¹⁰ in the context of low-density hole drag in bilayer p-GaAs 2D systems. For small $k_F d$, backscattering effects in Coulomb drag, which are unimportant for $k_F d \gg 1$, become important.

On the other hand, our numerical results also show

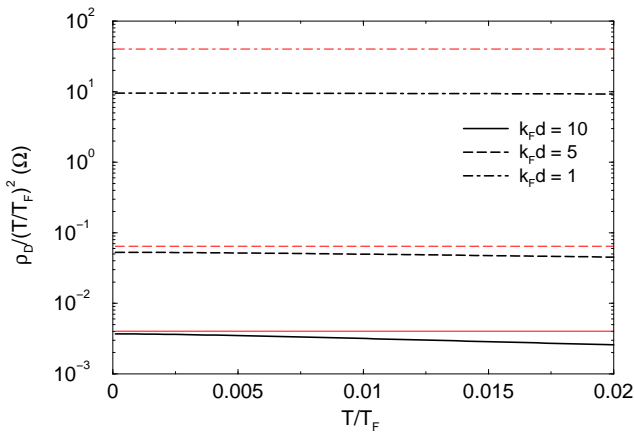


FIG. 2: (Color online) $\rho_D / (T/T_F)^2$ as a function of T/T_F for Coulomb drag between two identical extrinsic graphene sheets, with values of $k_F d = 10$ (solid lines), 5 (dashed lines), and 1 (dot-dashed lines). Numerical results are indicated with bold (black) lines and analytical results Eq. (12) with thin (grey/red) lines. The analytical results become an increasingly accurate approximation to the full numerical results with increasing $k_F d$ (i.e. increasing n or d).

that the temperature dependence of ρ_D remains very close to T^2 within a wide range of temperatures for typical experimental values of d and n (e.g. $k_F d = 5$ with $n = 5 \times 10^{11} \text{cm}^{-2}$ and $d \simeq 400 \text{\AA}$). The ratio of the Fermi temperature for graphene to that for regular 2DEG with parabolic spectrum (with effective mass m) is $T_F(\text{graphene})/T_F(2\text{DEG}) = mv/\hbar\sqrt{\pi n}$, so for low densities e.g. $n = 10^{11} \text{cm}^{-2}$, $T_F = 430 \text{K}$ for graphene can be larger by an order of magnitude than $T_F = 42 \text{K}$ for GaAs 2DEG, and the temperature dependence of ρ_D for graphene drag therefore remains very closely T^2 up to about several tens of kelvin where the low temperature regime $T \ll T_F$ still remains valid, whereas for drag in regular 2DEG systems departure from the T^2 dependence of ρ_D typically occurs at $T \lesssim 10 \text{K}$. The drag resistivity is calculated numerically for various values of d and n and higher values of temperature up to $T = 0.2T_F$ (Fig. 3); ρ_D is seen to grow slower and slower than T^2 as temperature increases. Similar dependence on temperature is also observed for drag in regular 2DEG bilayer systems before T reaches $\gtrsim 0.2T_F$, beyond which ρ_D/T^2 starts to increase due to plasmon enhancement to the Coulomb drag in graphene bilayer systems in the following.

In regular 2D bilayer systems, enhancement to the drag resistivity due to coupled plasmon modes comes into play with increasing temperature¹¹. There exist two plasmon modes, the so-called optic and acoustic modes, for which the electrons on the two layers move collectively in phase and out of phase, respectively, with each other. The energy dispersion lines for these plasmon modes lie above the electron-hole excitation continuum (i.e., the region of ω vs. q where the imaginary part of the polarizability is

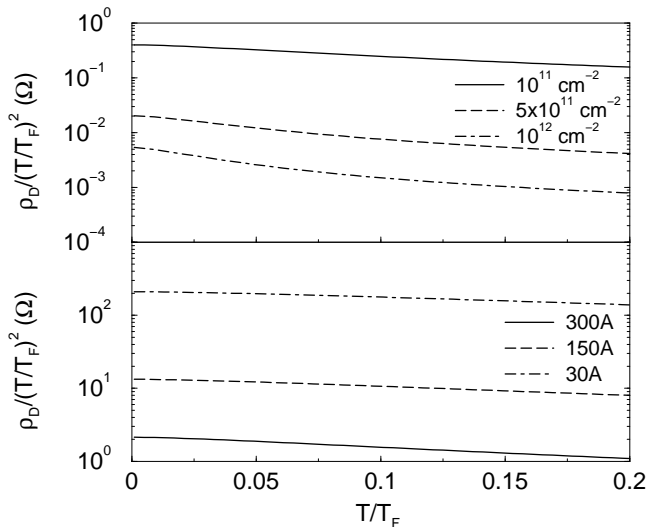


FIG. 3: $\rho_D / (T/T_F)^2$ vs. T/T_F for higher values of T up to $0.2T_F$. Upper panel: for fixed interlayer distance $d = 500 \text{\AA}$ and different values of density $n = 10^{11} \text{cm}^{-2}$ (solid line), $5 \times 10^{11} \text{cm}^{-2}$ (dashed line), 10^{12}cm^{-2} (dot-dashed line), corresponding to $T_F = 431 \text{K}$, 963K , 1361K respectively; lower panel: for fixed density $n = 10^{11} \text{cm}^{-2}$ and different values of interlayer distance $d = 300 \text{\AA}$ (solid line), 150\AA (dashed line) and 30\AA (dot-dashed line).

non-zero, $\text{Im}\Pi(q, \omega) \neq 0$) at zero temperature, and are not excited at low temperatures. They can be excited, however, at higher temperatures when the electron-hole excitation continuum occupies higher values of the excitation energy ω , a consequence of the increasing gradient with increasing momentum k in the parabolic energy dispersion relation. Absorption or emission of a plasmon can occur when the electron-hole excitation continuum starts to overlap with the plasmon dispersion. On the other hand for graphene, because the gradient of the linear dispersion relation is constant, increasing temperature does not increase the range of the possible intraband excitation energies, the electron-hole excitation continuum being always bounded by $\omega < vq$. This means that the plasmon excitation energy will always be out of reach from the intraband excitation channel at all temperatures. However, the case is different with the interband excitation, for which the electron-hole excitation continuum overlaps already at $T = 0$ with the plasmon dispersion at about⁴ $\omega \gtrsim \varepsilon_F$. This means that plasmon-induced enhancement of the drag resistivity in graphene occurs, solely due to interband transitions, at a temperature $T \gtrsim T_F$; whereas for regular 2D systems plasmon-induced enhancement occurs already before T reaches T_F (at about $T \simeq 0.5T_F$).

V. CONCLUSION

In conclusion, we have formulated the Coulomb drag problem for graphene bilayers. The drag resistivity is

zero for intrinsic graphene. For extrinsic graphene, the interband contribution to the drag due to electron-hole excitations is suppressed at low temperatures, and the Coulomb drag is due predominantly to the intraband contribution near the Fermi surface in the conduction band. We have obtained exact analytical results at $T = 0$ for both intraband and interband contributions to the non-linear susceptibility, and obtained the drag resistivity numerically. We have also derived an approximate analytical result for the drag resistivity valid for low temperatures, high density and/or large interlayer separation. We find both similarities and differences for the graphene drag resistivity compared with that for regular 2DEG with quadratic energy spectrum. At low temperatures, graphene drag resistivity exhibits the same temperature, bilayer distance and density dependences as regular 2D systems. For low densities $n \lesssim 10^{11} \text{cm}^{-2}$, the low temperature regime where the T^2 dependence of the drag resistivity holds extends by an order of magnitude that for regular 2D systems, as the Fermi temperature is higher for the same carrier density in graphene than in regular 2D systems. In contrast to regular 2D bilayer systems, there is no contribution to plasmon-induced enhancement of the drag resistivity due to intraband excitations, and the only contribution to plasmon-induced enhance-

ment comes from interband excitations, which occur at temperatures $T \gtrsim \varepsilon_F$. The coupled plasmon modes in graphene bilayer systems can therefore be probed experimentally with drag resistivity measurements at high enough temperatures or at low densities.

Finally, we comment on the possible effect of disorder which has been argued¹² to be important for substrate-mounted graphene monolayers in the low carrier density regime. In particular, the low-density graphene monolayers will be dominated¹² by spatial inhomogeneities associated with electron-hole puddles induced by the charged impurities in the substrate. In the presence of such density inhomogeneity, the Coulomb drag in the low-density regime may deviate substantially from our theory based on the spatially uniform carrier density (in each layer) model. In particular, there could be large drag fluctuations including even negative drag in this low-density regime.

VI. ACKNOWLEDGEMENT

This work is supported by US-ONR.

¹ K.S. Novoselov, *et al.*, Nature **438**, 197 (2005); Y. Zhang, *et al.*, Nature **438**, 201 (2005).

² A. Bostwick, *et al.*, Nat. Phys. **3**, 36 - 40 (2007)

³ S. Das Sarma, E.H. Hwang and W.-K. Tse, Phys. Rev. B **75**, 121406 (2007).

⁴ E.H. Hwang and S. Das Sarma, cond-mat/0610561; Phys. Rev. B (in press).

⁵ T.J. Gramila, *et al.*, Phys. Rev. Lett. **66**, 1216 (1991).

⁶ A.-P. Jauho and H. Smith, Phys. Rev. B **47**, 4420 (1993).

⁷ A. Kamenev and Y. Oreg, Phys. Rev. B **52**, 7516 (1995).

⁸ K. Flensberg, *et al.*, Phys. Rev. B **52**, 14761 (1995).

⁹ W.-K. Tse and S. Das Sarma, Phys. Rev. B **75**, 045333 (2007).

¹⁰ E.H. Hwang, *et al.*, Phys. Rev. Lett. **90**, 086801 (2003).

¹¹ K. Flensberg and B. Y.-K. Hu, Phys. Rev. Lett. **73**, 3572 (1994); Phys. Rev. B **52**, 14796 (1995).

¹² E.H. Hwang, S. Adam and S. Das Sarma, cond-mat/0610157; Phys. Rev. Lett. (in press).